

## JK PHOTOMETRY OF BRIGHT GIANTS IN NGC6712

JAE-MANN KYEONG<sup>1</sup> AND YONG-IK BYUN<sup>2</sup>

<sup>1</sup>Korea Astronomy Observatory, Daejeon 305-348, Korea

jman@hanul.issa.re.kr

<sup>2</sup>Department of Astronomy and Center for Space Astrophysics, Yonsei University, Seoul 120-749, Korea

byun@darksky.yonsei.ac.kr

(Received Sep. 25, 1998; Accepted Oct. 16, 1998)

### ABSTRACT

With a large format near-infrared camera at the 2.2-m telescope on Mauna Kea Observatory, we performed *JK* near-infrared observations for the metal rich globular cluster NGC6712. This cluster lies near the galactic plane and therefore suffers heavy reddening. We present the near-infrared color-magnitude diagram and also derive the metallicity ( $[Fe/H] \sim -0.96 \pm 0.27$ ) as well as its distance modulus ( $(m - M) \sim 13.42 \pm 0.12$ ).

*Key Words* : near-infrared photometry, metallicity, globular cluster, NGC6712

### I. INTRODUCTION

With their old age, globular clusters in our Galaxy provide valuable tool to understand the formation and evolution of the Galaxy. Some of the globular clusters, however, lie near the galactic plane and therefore it is very difficult to measure the fundamental parameters such as age, metallicity, and distance with accuracy. This is largely due to the significant reddening and its differential reddening as well as field star contamination. All of these cause scatter in color-magnitude diagrams (CMD) usually constructed with information obtained in visible wavelengths. Metal rich globular clusters in particular tend to lie near the crowded and heavily reddened low galactic latitude fields. The heavy reddening and scatter also complicates the effort to study the photometric properties of stars fainter than the horizontal branch (Armandroff & Zinn 1988). The problems caused by reddening can be easily overcome if the observations are made in near-infrared. Frogel *et al*(1983), for instance, performed near-infrared aperture photometry of evolved stars in a large sample of metal-rich and metal-poor globular clusters. However, because of the low observation efficiency of single element photometer, his study was restricted to small number of bright giant stars in each cluster. Kuchinski *et al*(1995) used near-IR array data of this cluster for calibrating the relation between the slope of giant branch and metallicity as a standard candle.

We are running a program to observe star clusters in low galactic latitude in near-infrared. So, Kyeong *et al* derived the metallicity of NGC6535 in the near-infrared as the first effort. This paper is a partial result of our on-going effort. NGC6712 ( $l=25.3^\circ$ ,  $b=-4.3^\circ$ ) is one of such low galactic latitude globular cluster suffering from reddening problem. Most X-ray clusters are known to have very strong concentration of stellar density toward the center, however NGC6712 does not have such a strong central concentration(Cudworth 1988).

**Table 1.** Journal of NGC6712 Observation.

Date	Field	Location	Exposure	FWHM
July 30 1993	sky	30' south	7x3sec(J)	
	NGC6712	Center	7x3sec(J)	1.1''
	sky	30' south	7x3sec(J)	
	sky	30' south	7x3sec(K')	
	NGC6712	Center	7x3sec(K')	1.0''
	sky	30' south	7x3sec(K')	

Although a number of X-ray observations have been performed for NGC6712, however optical observations with modern CCD technology have been not made yet. The available CMD consists of photographic data sets. Sandage & Smith (1966), who constructed this CMD, found a red giant branch with a shallow slope of a moderately metal-rich cluster. Its horizontal branch have stars well distributed on both sides of the RR Lyrae region, but with dominant population toward the red end. According to their estimates, color excess was  $E(B-V)=0.48$  and distance was  $d=6.75\text{kpc}$ . More recently, Frogel (1985) observed several bright giants and variables in this cluster using a near-IR photometer. He derived  $[Fe/H]=-0.92$  using equations (7a) and (7b) of Frogel *et al*(1983), which was in general agreement with several optical studies(for example, Zinn & West(1985)'s -1.01).

With a modern two-dimensional near-infrared camera of large array format, we observed this cluster in *J* and *K* bands. The details of observations and calibrations are given in section 2. This paper also contains a near-infrared CMD constructed with our data, which is given in section 3. We estimate the metallicity and

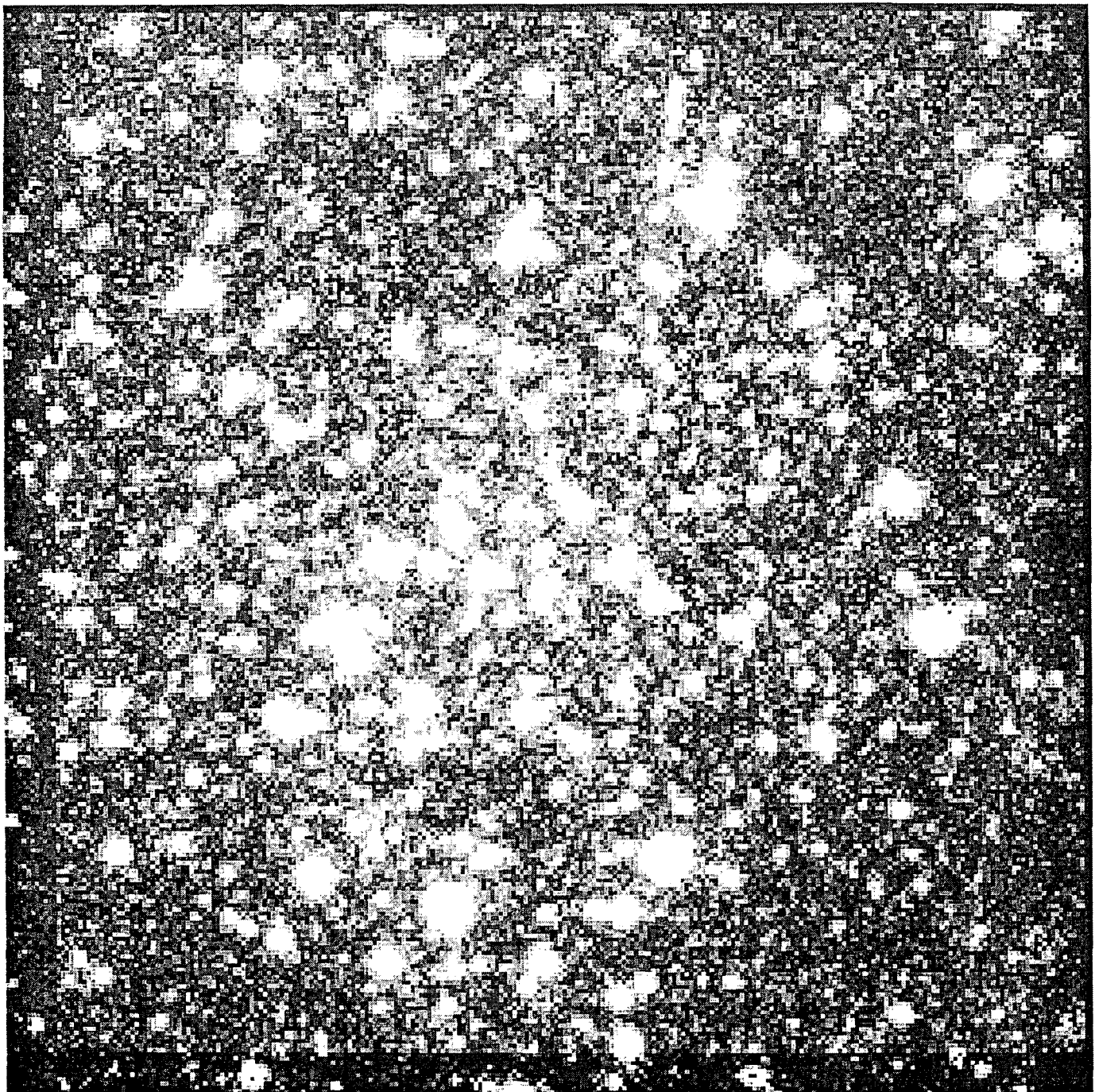


**Fig. 1.**— Image of NGC6712 central region in *J* band(*left*) *K* band(*right*). Exposure time is 3 second and field of view is about 1.6 arcmin. North is to the left, east is to the top.

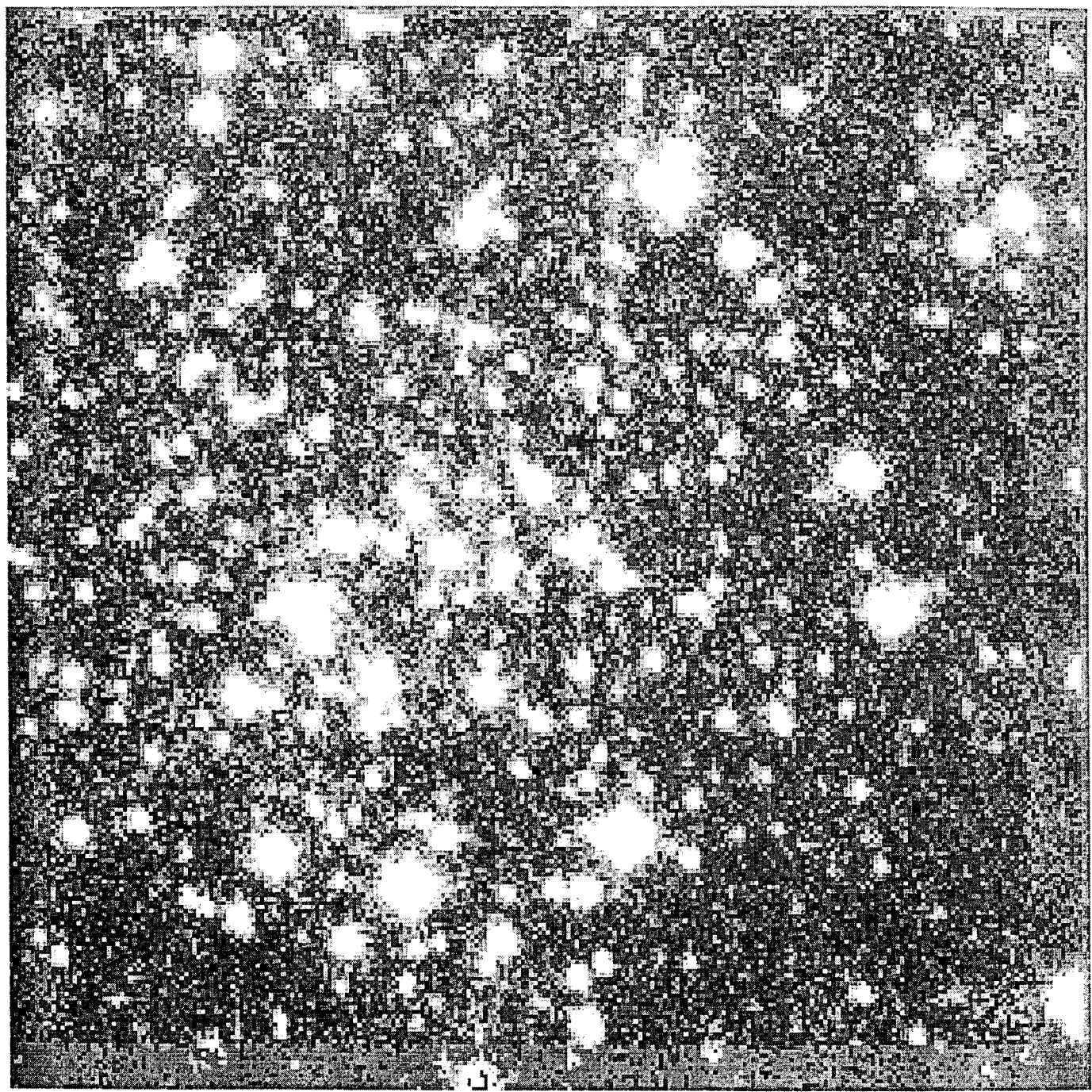


Fig. 1. - Continued

**Table 2.** JK Photometric data of NGC6712

ID	X	Y	J	$\sigma_J$	K	$\sigma_K$	ID	X	Y	J	$\sigma_J$	K	$\sigma_K$
1	175.64	35.57	14.541	0.049	14.551	0.179	39	149.60	114.60	15.443	0.074	15.002	0.117
2	261.84	38.52	15.803	0.166	16.208	0.166	40	80.74	114.82	15.579	0.099	15.537	0.201
3	242.60	39.91	16.285	0.113	16.296	0.314	41	256.86	114.84	14.696	0.050	14.116	0.060
4	138.46	44.91	15.375	0.080	15.062	0.132	42	212.23	116.12	13.656	0.162	12.972	0.056
5	143.00	49.03	15.986	0.134	15.787	0.184	43	176.95	116.36	14.018	0.049	13.330	0.057
6	68.43	49.63	15.334	0.125	15.393	0.125	44	186.49	116.55	16.516	0.116	15.974	0.293
7	265.84	51.48	15.351	0.057	15.004	0.100	45	75.67	117.90	16.634	0.198	16.206	0.283
8	203.63	59.09	14.846	0.065	14.549	0.094	46	240.46	118.67	14.711	0.070	14.063	0.053
9	196.65	59.75	16.252	0.107	15.411	0.144	47	268.48	119.00	15.394	0.053	15.525	0.177
10	54.95	60.42	13.976	0.058	13.421	0.065	48	83.12	121.60	16.280	0.119	16.014	0.282
11	122.02	63.78	11.750	0.041	10.981	0.043	49	155.10	122.79	11.994	0.047	11.126	0.037
12	111.43	64.72	16.364	0.101	15.247	0.109	50	130.23	125.17	11.154	0.053	10.117	0.036
13	104.98	71.01	17.256	0.223	16.008	0.256	51	72.48	131.38	15.840	0.109	15.353	0.186
14	88.93	71.75	14.009	0.040	13.473	0.077	52	195.10	129.95	13.595	0.050	12.874	0.040
15	228.42	71.82	16.051	0.104	15.460	0.128	53	279.95	130.96	15.013	0.081	14.347	0.088
16	85.01	74.15	14.206	0.055	13.501	0.049	54	273.40	130.97	14.515	0.070	13.899	0.049
17	109.51	75.32	16.309	0.095	16.097	0.220	55	124.41	137.52	16.879	0.211	15.644	0.181
18	186.68	75.73	16.124	0.099	15.525	0.122	56	221.79	138.54	16.575	0.153	16.031	0.241
19	171.39	76.45	13.395	0.043	12.628	0.062	57	238.54	140.04	16.266	0.173	15.927	0.175
20	120.48	78.51	14.506	0.052	13.962	0.066	58	135.95	140.07	15.892	0.092	16.085	0.284
21	237.51	81.79	16.255	0.138	15.841	0.200	59	251.15	141.53	10.664	0.046	9.588	0.056
22	84.46	84.69	15.116	0.067	14.843	0.102	60	121.63	142.03	15.011	0.071	14.250	0.087
23	161.97	87.57	16.536	0.163	16.072	0.278	61	74.63	142.73	16.664	0.194	15.798	0.233
24	173.53	88.29	15.058	0.062	15.094	0.118	62	225.57	143.34	15.934	0.107	15.251	0.104
25	187.99	88.74	10.079	0.032	8.923	0.044	63	61.00	145.67	13.919	0.036	13.360	0.045
26	224.51	90.55	15.228	0.065	14.675	0.074	64	261.99	147.10	15.075	0.064	14.636	0.087
27	119.29	90.67	13.882	0.058	13.228	0.045	65	209.95	147.41	14.158	0.061	13.620	0.060
28	84.80	93.55	17.272	0.312	16.569	0.431	66	105.78	153.36	15.780	0.110	15.564	0.136
29	204.14	97.46	14.423	0.056	13.713	0.049	67	94.39	155.18	15.859	0.101	15.216	0.151
30	174.60	99.76	15.039	0.099	14.744	0.107	68	218.42	158.39	16.871	0.149	16.197	0.231
31	192.58	100.67	14.126	0.042	13.681	0.063	69	120.12	159.11	11.495	0.033	10.584	0.044
32	128.53	102.14	14.039	0.051	13.563	0.049	70	262.90	162.22	15.711	0.107	16.070	0.265
33	209.37	103.09	15.981	0.100	15.300	0.098	71	89.08	170.14	13.776	0.043	13.112	0.043
34	81.42	104.31	16.778	0.174	16.371	0.440	72	182.08	174.38	16.377	0.142	15.845	0.196
35	189.47	104.89	16.200	0.114	15.248	0.141	73	199.39	172.98	13.872	0.052	13.342	0.049
36	97.99	109.03	17.154	0.283	16.110	0.232	74	210.34	173.46	13.781	0.041	13.150	0.034
37	103.50	111.37	15.701	0.095	15.793	0.238	75	56.41	178.61	15.982	0.114	16.176	0.317

**Table 2.** - Continued

ID	X	Y	J	$\sigma_J$	K	$\sigma_K$	ID	X	Y	J	$\sigma_J$	K	$\sigma_K$
38	190.44	113.02	16.034	0.131	15.470	0.116	76	132.84	184.98	15.848	0.092	15.395	0.163
77	193.42	180.83	16.370	0.136	15.537	0.147	115	124.86	248.29	17.040	0.224	16.591	0.434
78	184.41	184.13	14.365	0.056	13.746	0.061	116	103.91	249.48	15.492	0.071	14.771	0.128
79	146.43	184.12	15.473	0.117	14.703	0.112	117	154.96	252.20	16.072	0.095	15.673	0.147
80	161.99	183.07	15.099	0.054	14.431	0.094	118	145.16	252.45	14.018	0.055	13.418	0.060
81	223.94	185.44	16.537	0.168	16.347	0.329	119	268.51	253.63	15.084	0.120	14.496	0.100
82	209.08	185.96	15.787	0.090	15.534	0.134	120	218.58	254.74	15.422	0.078	15.136	0.104
83	70.92	187.99	17.028	0.222	16.538	0.473	121	190.02	258.93	14.813	0.072	14.640	0.081
84	180.47	189.53	14.968	0.055	14.529	0.061	122	116.15	261.49	13.503	0.048	12.926	0.042
85	187.85	190.66	13.930	0.058	13.238	0.044	123	57.40	262.52	15.889	0.093	15.652	0.217
86	57.95	191.24	14.468	0.058	13.795	0.058	124	140.68	265.23	16.670	0.181	16.048	0.223
87	63.75	192.79	16.090	0.200	15.571	0.187	125	276.55	267.51	15.752	0.091	15.606	0.187
88	44.46	192.41	14.370	0.101	13.868	0.072	126	185.05	267.67	15.575	0.123	15.507	0.165
89	196.08	192.82	16.749	0.187	16.070	0.280	127	92.42	271.80	11.111	0.062	10.035	0.074
90	133.98	193.62	13.651	0.036	12.980	0.034	128	111.36	272.58	14.687	0.056	14.446	0.108
91	75.34	200.11	13.720	0.062	12.920	0.041	129	71.50	274.12	16.089	0.120	16.052	0.336
92	134.95	201.32	16.273	0.131	15.724	0.160	130	106.51	42.91	15.646	0.086	14.651	0.108
93	185.51	206.12	13.873	0.127	12.869	0.037	131	106.08	45.88	15.405	0.082	15.004	0.147
94	192.49	206.20	16.881	0.229	16.417	0.323	132	168.76	49.18	15.658	0.054	14.944	0.138
95	177.86	208.51	14.590	0.065	13.835	0.059	133	243.81	51.93	13.635	0.076	13.158	0.063
96	238.51	209.99	14.958	0.051	14.417	0.067	134	136.13	53.34	14.100	0.047	13.501	0.060
97	93.07	210.16	14.209	0.066	13.382	0.057	135	176.72	55.40	12.843	0.038	12.517	0.051
98	257.93	210.71	14.703	0.073	14.041	0.080	136	155.14	58.20	14.031	0.043	13.440	0.052
99	117.05	211.06	16.657	0.156	15.463	0.128	137	143.65	63.33	14.897	0.051	14.474	0.103
100	77.38	211.86	16.057	0.111	15.469	0.191	138	159.02	63.83	12.195	0.040	11.251	0.039
101	112.36	214.70	14.004	0.060	13.527	0.045	139	49.85	64.29	14.698	0.067	14.599	0.042
102	230.92	221.71	15.120	0.098	14.465	0.069	140	269.68	65.22	16.025	0.095	15.840	0.291
103	176.89	222.26	15.129	0.080	14.668	0.093	141	277.93	65.84	16.419	0.135	16.158	0.322
104	140.41	224.83	15.651	0.084	15.204	0.106	142	167.91	67.60	16.914	0.186	16.075	0.296
105	257.48	227.43	15.753	0.079	15.162	0.131	143	261.68	71.37	15.845	0.068	15.196	0.140
106	107.04	230.66	15.933	0.094	15.206	0.119	144	96.70	69.22	12.756	0.049	11.820	0.054
107	195.93	231.57	15.277	0.060	14.418	0.093	145	159.78	75.23	14.449	0.053	13.980	0.052
108	55.51	235.08	14.180	0.056	13.957	0.050	146	178.56	76.40	12.464	0.042	11.701	0.040
109	178.92	232.20	16.004	0.112	15.257	0.153	147	78.68	78.56	16.135	0.086	16.096	0.251
110	170.01	234.77	16.668	0.177	16.335	0.325	148	203.52	83.51	13.762	0.050	13.022	0.051
111	280.38	235.06	11.450	0.072	10.148	0.044	149	105.05	84.25	11.020	0.034	9.957	0.052
112	254.89	239.49	14.524	0.059	13.808	0.068	150	198.86	85.80	15.706	0.071	14.921	0.159

**Table 2.** - Continued

ID	X	Y	J	$\sigma_J$	K	$\sigma_K$	ID	X	Y	J	$\sigma_J$	K	$\sigma_K$
113	143.59	241.04	15.981	0.099	15.838	0.224	151	215.14	89.44	15.415	0.072	14.948	0.109
114	176.30	245.41	15.836	0.086	15.379	0.138	152	178.88	90.42	14.905	0.045	13.910	0.062
153	73.46	92.17	13.932	0.048	13.297	0.046	191	144.85	137.74	15.087	0.096	14.419	0.059
154	135.54	92.25	15.824	0.114	15.595	0.183	192	89.51	139.10	14.057	0.071	13.328	0.045
155	140.04	92.36	13.968	0.048	13.172	0.044	193	185.67	139.16	15.845	0.067	15.563	0.186
156	123.85	93.71	14.460	0.054	14.214	0.071	194	193.51	142.32	15.376	0.081	15.642	0.231
157	101.22	94.26	15.117	0.062	14.716	0.089	195	165.89	142.59	16.624	0.165	15.573	0.214
158	114.70	95.62	14.283	0.050	13.535	0.055	196	106.82	142.73	12.759	0.037	12.054	0.031
159	144.62	97.75	15.575	0.073	14.787	0.082	197	111.15	144.24	12.112	0.036	11.324	0.038
160	243.29	99.82	13.961	0.058	13.352	0.062	198	149.92	144.51	14.032	0.048	13.428	0.059
161	114.76	103.68	16.137	0.102	15.593	0.166	199	142.47	144.90	13.931	0.062	13.142	0.042
162	162.96	104.74	13.964	0.040	13.608	0.035	200	93.41	148.02	15.444	0.108	15.173	0.163
163	253.64	106.43	16.516	0.144	15.905	0.197	201	190.34	148.54	14.522	0.073	14.133	0.066
164	76.63	107.59	13.938	0.031	13.458	0.047	202	46.81	153.44	13.627	0.045	13.321	0.080
165	61.10	107.69	16.244	0.172	16.059	0.262	203	145.53	155.18	11.880	0.063	10.880	0.042
166	92.95	110.54	13.991	0.049	13.495	0.050	204	102.15	153.66	15.845	0.101	14.997	0.108
167	108.32	112.85	16.779	0.235	16.185	0.371	205	177.42	153.95	13.909	0.054	13.290	0.062
168	225.86	115.29	13.075	0.059	12.433	0.054	206	110.20	154.21	15.720	0.079	15.123	0.110
169	167.99	115.44	13.141	0.057	12.640	0.040	207	211.84	156.17	15.167	0.070	14.681	0.119
170	88.40	115.76	14.803	0.038	14.123	0.077	208	270.86	157.04	15.350	0.098	15.037	0.124
171	140.25	116.10	16.354	0.150	15.960	0.213	209	91.28	157.76	17.182	0.304	16.693	0.443
172	133.80	116.69	13.938	0.037	13.314	0.063	210	178.65	158.25	12.314	0.049	11.528	0.042
173	68.58	117.12	14.748	0.061	14.008	0.065	211	61.73	158.65	14.289	0.058	13.738	0.051
174	69.45	123.25	15.136	0.062	14.495	0.076	212	71.74	160.25	13.839	0.055	13.269	0.047
175	57.49	117.30	12.725	0.054	12.022	0.041	213	96.45	160.52	14.618	0.092	14.527	0.073
176	164.01	118.30	14.958	0.067	14.336	0.065	214	127.29	160.71	14.199	0.047	13.426	0.068
177	96.40	123.00	12.414	0.057	11.453	0.049	215	152.45	161.23	16.247	0.132	15.474	0.233
178	105.32	120.76	14.037	0.064	13.364	0.060	216	192.25	163.66	16.679	0.159	16.377	0.339
179	122.76	121.50	15.371	0.059	14.962	0.114	217	75.09	163.89	13.950	0.036	13.353	0.043
180	186.54	123.10	15.671	0.078	15.068	0.125	218	267.63	165.84	16.173	0.086	15.535	0.223
181	188.40	125.64	16.068	0.091	15.895	0.172	219	178.04	166.59	14.228	0.056	13.610	0.040
182	226.89	123.29	15.001	0.078	14.438	0.080	220	78.09	168.18	15.434	0.130	15.026	0.118
183	235.20	128.81	14.476	0.049	13.900	0.058	221	234.12	168.69	15.470	0.078	15.046	0.136
184	178.01	127.42	13.589	0.044	12.979	0.059	222	157.06	169.23	14.850	0.061	14.212	0.071
185	105.41	129.84	14.740	0.073	14.056	0.077	223	135.17	169.24	13.763	0.063	13.298	0.042
186	142.37	129.39	16.435	0.132	15.805	0.212	224	146.10	170.37	16.826	0.227	15.370	0.159
187	221.14	130.75	14.145	0.050	13.341	0.047	225	167.15	170.56	11.773	0.056	10.654	0.049

Table 2. - Continued

ID	X	Y	J	$\sigma_J$	K	$\sigma_K$	ID	X	Y	J	$\sigma_J$	K	$\sigma_K$
188	115.73	135.10	12.132	0.052	11.224	0.051	226	191.83	171.85	14.180	0.046	13.661	0.061
189	158.26	135.50	15.381	0.080	14.734	0.086	227	46.02	179.24	13.840	0.063	13.650	0.071
190	218.24	136.09	15.472	0.069	15.187	0.123	228	143.01	173.23	14.931	0.076	14.226	0.054
229	139.22	176.63	13.909	0.057	13.123	0.047	267	116.79	226.58	16.737	0.140	16.063	0.259
230	78.95	178.80	14.054	0.032	13.596	0.045	268	283.96	227.32	14.149	0.456	13.042	0.066
231	110.62	179.99	14.296	0.067	13.450	0.063	269	250.70	227.26	16.437	0.099	15.865	0.191
232	213.19	180.31	13.891	0.050	13.063	0.032	270	151.75	230.54	11.861	0.051	10.934	0.060
233	281.46	188.62	15.577	0.082	15.065	0.106	271	160.55	230.65	13.712	0.047	12.992	0.052
234	219.51	186.54	17.441	0.312	16.646	0.460	272	118.61	234.23	14.959	0.055	14.478	0.061
235	98.36	188.31	12.349	0.054	11.516	0.050	273	96.39	238.04	16.354	0.140	16.007	0.240
236	141.67	189.53	15.462	0.069	14.813	0.098	274	83.20	238.18	13.080	0.071	14.687	0.528
237	207.71	191.52	14.838	0.057	14.357	0.115	275	83.20	238.18	13.440	0.071	12.823	0.085
238	172.40	194.44	16.194	0.121	15.504	0.173	276	132.16	238.55	16.119	0.146	15.595	0.132
239	94.04	192.08	15.148	0.062	14.379	0.122	277	128.92	239.88	15.990	0.079	15.248	0.116
240	218.05	194.04	14.336	0.044	13.671	0.049	278	48.25	239.36	13.709	0.049	13.504	0.093
241	180.18	195.60	12.538	0.063	11.786	0.057	279	104.89	240.01	13.891	0.040	13.263	0.043
242	239.35	195.86	14.824	0.067	14.110	0.061	280	199.67	240.70	9.896	0.049	8.802	0.030
243	190.84	195.95	16.199	0.123	15.765	0.200	281	157.53	240.83	13.977	0.056	13.368	0.054
244	162.93	199.25	14.302	0.041	13.600	0.055	282	64.67	245.40	16.687	0.199	15.773	0.159
245	188.94	202.26	14.177	0.047	13.527	0.048	283	263.04	245.59	12.129	0.048	11.248	0.048
246	225.83	202.79	12.948	0.032	12.116	0.037	284	265.68	246.95	12.228	0.053	11.226	0.024
247	282.88	203.74	15.041	0.079	14.392	0.068	285	183.82	248.77	15.861	0.088	15.132	0.077
248	58.67	205.04	15.458	0.066	15.157	0.080	286	188.96	249.61	13.318	0.041	12.401	0.042
249	274.40	203.98	14.229	0.078	13.393	0.070	287	280.53	255.14	12.961	0.087	11.910	0.044
250	240.01	204.45	16.511	0.147	16.054	0.257	288	63.10	255.97	15.942	0.146	15.681	0.167
251	126.45	210.73	12.905	0.057	12.016	0.039	289	258.89	256.31	13.902	0.045	13.443	0.093
252	227.21	207.64	14.719	0.064	14.311	0.069	290	228.62	261.07	12.749	0.054	11.989	0.027
253	146.30	208.12	15.558	0.063	15.147	0.156	291	104.33	261.15	15.960	0.079	15.345	0.153
254	83.10	208.91	14.334	0.069	13.550	0.064	292	73.09	261.75	13.988	0.048	13.409	0.074
255	55.71	209.72	14.323	0.051	13.714	0.075	293	190.82	264.04	13.936	0.043	13.383	0.047
256	262.51	210.22	14.186	0.060	13.709	0.063	294	67.17	269.25	15.493	0.066	15.044	0.110
257	184.87	213.70	14.720	0.064	13.993	0.058	295	191.68	269.03	13.943	0.045	13.392	0.053
258	223.04	216.80	12.805	0.051	11.955	0.041	296	138.63	269.11	15.170	0.109	14.713	0.119
259	179.83	215.54	15.291	0.088	14.636	0.096	297	143.47	271.86	15.161	0.063	15.093	0.167
260	73.19	219.86	13.950	0.050	13.164	0.077	298	222.33	270.23	16.576	0.170	15.997	0.240
261	279.19	218.90	13.878	0.058	12.952	0.041	299	105.61	270.51	14.939	0.057	14.533	0.089
262	164.59	219.63	16.087	0.113	16.081	0.254	300	195.85	275.43	14.657	0.060	14.201	0.067

**Table 2.** - Continued

ID	X	Y	J	$\sigma_J$	K	$\sigma_K$	ID	X	Y	J	$\sigma_J$	K	$\sigma_K$
263	165.79	222.78	15.800	0.087	15.022	0.067	301	265.27	277.73	15.007	0.088	14.580	0.077
264	77.93	224.43	12.534	0.083	12.022	0.050	302	186.47	278.14	15.607	0.082	16.265	0.386
265	185.87	225.07	12.431	0.043	12.332	0.035	303	125.43	279.66	12.294	0.067	11.525	0.077
266	222.02	225.26	15.324	0.082	15.229	0.133	304	208.64	43.75	16.064	0.115	15.992	0.219
305	178.96	44.24	12.058	0.040	11.340	0.040	343	105.52	189.68	14.423	0.050	13.600	0.068
306	218.23	49.43	16.200	0.137	16.199	0.321	344	106.66	192.06	15.466	0.066	14.377	0.093
307	120.74	53.36	15.478	0.078	14.816	0.082	345	157.85	190.95	13.670	0.043	13.067	0.038
308	136.84	76.75	10.134	0.033	9.003	0.045	346	89.65	200.01	14.037	0.062	13.483	0.052
309	248.29	81.88	15.046	0.061	14.460	0.071	347	117.67	194.52	15.883	0.128	15.222	0.152
310	143.36	87.43	14.483	0.060	13.774	0.076	348	52.88	195.89	15.719	0.096	15.226	0.120
311	221.39	103.00	15.317	0.069	14.624	0.076	349	199.68	197.72	15.316	0.060	14.302	0.064
312	46.65	107.45	15.993	0.104	15.896	0.217	350	150.13	205.35	14.464	0.055	13.784	0.050
313	275.16	110.22	15.960	0.121	15.301	0.099	351	153.22	206.31	14.050	0.068	13.161	0.066
314	224.47	118.29	13.970	0.065	13.433	0.050	352	155.53	205.66	13.516	0.057	12.662	0.046
315	98.15	118.93	13.127	0.043	12.295	0.043	353	248.32	199.59	15.925	0.155	15.540	0.156
316	175.17	121.96	17.008	0.273	16.569	0.396	354	106.35	200.03	15.207	0.146	14.561	0.063
317	159.96	124.61	16.195	0.156	15.218	0.149	355	216.69	204.85	15.415	0.085	14.939	0.139
318	51.01	128.15	14.433	0.049	14.365	0.083	356	210.75	205.65	16.369	0.123	15.461	0.151
319	78.56	128.57	13.977	0.057	13.638	0.087	357	206.04	204.69	14.311	0.043	13.949	0.062
320	78.23	134.17	14.926	0.058	14.146	0.081	358	160.28	206.10	15.802	0.120	15.316	0.167
321	156.15	129.50	13.857	0.052	13.254	0.039	359	128.69	206.63	14.062	0.046	13.335	0.058
322	178.28	131.37	15.067	0.062	14.905	0.120	360	174.16	209.56	14.990	0.060	14.689	0.088
323	204.70	135.12	16.522	0.165	16.264	0.326	361	103.03	213.29	16.818	0.164	15.862	0.251
324	202.65	143.00	14.019	0.040	13.342	0.065	362	99.28	216.30	13.194	0.066	12.325	0.045
325	85.30	139.76	15.443	0.096	15.032	0.124	363	101.27	218.44	13.807	0.058	13.184	0.056
326	103.21	140.79	13.940	0.048	13.506	0.060	364	153.57	217.30	15.315	0.084	14.989	0.090
327	158.90	147.78	14.073	0.057	13.394	0.050	365	215.68	226.06	11.463	0.047	10.477	0.035
328	49.07	145.14	13.894	0.055	13.957	0.066	366	270.04	228.24	11.729	0.056	10.796	0.036
329	257.78	146.19	15.081	0.092	13.675	0.098	367	76.46	228.79	16.154	0.139	15.326	0.148
330	184.98	148.49	12.785	0.046	12.074	0.034	368	80.75	234.72	14.950	0.058	14.234	0.062
331	244.52	153.62	13.986	0.048	13.196	0.037	369	201.35	232.76	16.201	0.117	14.832	0.093
332	173.07	156.30	14.855	0.094	13.873	0.061	370	154.11	236.93	13.163	0.037	12.834	0.067
333	42.65	154.68	15.191	0.077	14.801	0.124	371	186.71	239.65	13.798	0.048	13.337	0.057
334	123.92	155.34	14.939	0.092	14.353	0.080	372	99.05	240.17	16.308	0.112	15.314	0.140
335	75.71	157.18	17.304	0.413	16.519	0.444	373	271.83	247.69	16.483	0.172	15.618	0.198
336	160.18	161.59	15.241	0.076	14.853	0.143	374	201.68	248.42	12.273	0.045	11.269	0.037
337	139.77	165.45	12.311	0.118	11.460	0.096	375	243.84	250.09	16.688	0.180	15.985	0.300

**Table 2.** - Continued

ID	X	Y	J	$\sigma_J$	K	$\sigma_K$	ID	X	Y	J	$\sigma_J$	K	$\sigma_K$
338	86.04	167.73	14.180	0.061	13.524	0.056	376	203.00	255.44	15.861	0.100	15.195	0.139
339	109.82	171.68	16.614	0.162	16.394	0.262	377	59.51	258.56	16.528	0.163	15.645	0.217
340	163.92	174.34	13.933	0.070	13.561	0.067	378	203.39	259.75	14.551	0.090	14.051	0.084
341	116.33	183.62	13.174	0.052	12.477	0.047	379	121.53	260.98	16.233	0.136	15.393	0.114
342	229.44	190.96	14.547	0.060	13.651	0.065	380	164.16	265.83	15.944	0.131	15.329	0.189
381	122.57	266.37	12.781	0.043	11.909	0.041	419	182.72	58.92	13.517	0.047	13.157	0.045
382	81.26	274.11	14.194	0.044	13.563	0.049	420	143.05	82.30	17.430	0.192	14.092	0.155
383	134.39	278.31	14.118	0.067	13.413	0.055	421	245.62	89.24	15.701	0.138	15.382	0.235
384	254.28	278.52	16.045	0.097	15.679	0.280	422	182.09	107.94	14.189	0.045	13.628	0.055
385	130.11	278.74	13.980	0.066	13.658	0.070	423	127.96	114.96	12.756	0.061	12.085	0.041
386	180.07	280.38	13.916	0.055	13.877	0.057	424	100.13	121.64	14.559	0.097	13.897	0.103
387	138.58	62.10	14.191	0.045	13.653	0.078	425	58.53	125.82	13.171	0.126	12.373	0.049
388	146.13	89.08	13.323	0.049	12.433	0.048	426	79.24	130.59	16.290	0.138	14.950	0.137
389	58.75	89.54	12.712	0.064	11.806	0.040	427	207.83	138.57	16.199	0.140	15.276	0.146
390	113.58	115.69	13.959	0.048	13.268	0.071	428	113.71	139.39	11.875	0.043	10.722	0.047
391	47.76	113.83	14.020	0.042	14.399	0.079	429	185.78	151.00	14.368	0.081	13.237	0.106
392	248.39	118.80	16.500	0.198	16.306	0.299	430	239.32	173.67	14.394	0.072	13.608	0.074
393	48.93	124.69	16.091	0.149	16.246	0.253	431	83.99	180.09	13.902	0.051	13.234	0.050
394	124.94	129.47	15.113	0.079	14.312	0.082	432	84.90	195.60	14.350	0.038	13.924	0.073
395	206.05	143.21	13.768	0.040	13.256	0.071	433	85.94	199.09	14.468	0.047	13.877	0.091
396	176.43	142.05	15.643	0.104	15.114	0.156	434	149.91	198.56	14.773	0.084	14.033	0.057
397	116.61	145.17	13.865	0.087	13.102	0.082	435	90.06	257.97	11.864	0.043	10.710	0.022
398	166.30	147.33	15.517	0.160	14.640	0.128	436	52.25	257.99	12.337	0.073	12.003	0.122
399	166.86	150.88	17.087	0.237	15.876	0.287	437	176.05	276.06	16.402	0.114	15.630	0.193
400	84.86	150.31	13.444	0.040	12.570	0.034	438	179.33	101.70	14.038	0.049	13.205	0.035
401	159.80	151.91	12.520	0.049	11.559	0.043	439	118.30	123.89	13.759	0.057	12.946	0.036
402	133.98	156.97	12.961	0.039	12.009	0.061	440	158.36	158.37	15.748	0.099	15.950	0.277
403	158.39	160.99	14.917	0.051	14.476	0.080	441	115.84	165.83	16.027	0.123	15.615	0.155
404	105.95	163.32	15.840	0.103	15.364	0.152	442	150.39	169.01	15.962	0.149	15.563	0.269
405	152.49	170.12	13.853	0.050	13.126	0.066	443	243.78	173.63	11.600	0.046	10.532	0.031
406	161.73	178.32	15.700	0.123	15.120	0.104	444	242.32	176.25	13.925	0.087	13.475	0.095
407	139.92	210.78	14.930	0.080	14.136	0.083	445	88.81	184.05	16.405	0.151	15.132	0.100
408	141.94	210.79	13.971	0.042	13.303	0.049	446	158.15	233.14	14.463	0.073	13.654	0.041
409	137.41	211.01	14.552	0.058	13.862	0.065	447	57.65	125.37	15.539	0.151	12.325	0.049
410	224.64	211.39	16.290	0.154	16.019	0.262	448	133.65	180.40	16.254	0.151	15.438	0.164
411	95.65	214.02	15.059	0.070	14.472	0.082	449	149.91	202.07	17.114	0.222	15.883	0.332
412	82.80	217.57	16.575	0.211	16.197	0.286	450	153.57	31.55	13.871	0.527	10.623	0.242

**Table 2.** - Continued

ID	X	Y	<i>J</i>	$\sigma_J$	<i>K</i>	$\sigma_K$	ID	X	Y	<i>J</i>	$\sigma_J$	<i>K</i>	$\sigma_K$
413	189.51	222.80	15.042	0.055	14.398	0.081	451	145.43	229.19	16.677	0.251	15.480	0.165
414	79.23	220.96	12.483	0.053	11.620	0.048	452	135.29	251.02	14.066	0.066	13.475	0.057
415	192.51	242.86	14.264	0.064	13.362	0.079	453	154.57	258.73	14.165	0.081	13.505	0.040
416	77.76	243.94	15.201	0.085	14.783	0.065	454	83.19	222.55	15.922	0.123	15.628	0.190
417	157.71	269.81	12.405	0.040	11.549	0.027	455	150.43	89.44	16.318	0.132	15.559	0.166
418	144.89	274.00	16.309	0.119	15.993	0.281							

distance modulus in section 4. Section 5 summarizes our results.

## II. OBSERVATIONS AND CALIBRATION

The observations were carried out with the University of Hawaii 2.2m telescope and its NICMOS3 infrared camera system during July 30 - 31 1993. The detailed observational techniques, data acquisition and reduction are almost identical to those presented in Kyeong *et al*(1997). Details of instrument characteristics are given in Hoddap *et al*(1992).

Our observations targeted the central region of NGC 6712. The usual procedure for near-infrared observations is to make consequent exposures in jitter pattern in order to estimate the level and structure of near-infrared background. However, the high density of stars in our field did not allow more efficient jitter observations. We instead chose a region about 30 arcmin away from the cluster center toward south. Jitter observations were made to this sky region before and after cluster exposures and used to eliminate the background flux from the cluster frames. The observation log, exposure time and FWHM of each cluster data frame are given in Table 1.

Data reduction has been done as follows. First, a median dark frame has been made using all dark exposures of the same exposure time. This dark frame was subtracted from each data frame and at the same time linearity correction has also been made. Second, for each cluster observation the corresponding background frame was constructed by median combining of sky exposures and subsequently subtracted from cluster frames. This makes the background level of cluster frame to zero, and make it suitable to apply dome flats. Dome flats are prepared separately by combining the differential images between flat images taken with and without lamp illumination. The flatfielding is done for all seven cluster exposures by dividing them with the normalized flatfield in each passband. Finally, the cluster exposures were aligned and averaged to create a final cluster image in each passband. The final processed images in *J* and *K* band are shown in Figure 1.

Stellar photometry was carried out using a well known point-spread-function fitting photometry algorithm called ALLSTAR. The version we used is a part of the IRAF/DAOPHOT photometry package (Stetson & Harris 1988). The instrumental magnitudes obtained by ALLSTAR were transformed using a formula we derived from the aperture photometry data of UKIRT standard stars. The color coefficients and zero points are identical to those given in Table 3 of Kyeong *et al* (1997). Fully transformed ALLSTAR *J* and *K* magnitudes for 455 stars are listed in Table 2 along with their positions and estimated errors.

## III. COLOR-MAGNITUDE DIAGRAMS

We present the (*K*,  $J - K$ ) CMD of NGC6712 in Fig. 2. In the CMD, the giant branch is well developed and clearly visible. The horizontal branch exists near  $K \sim 13.5$  mag. There is no discernible gap between the giant branch and horizontal branch, however the giant branch appears to have some clearance between its red giant branch and asymptotic giant branch. The general shape is the giant branch is linear with steep slope. It is much simpler than and different from the shape of optically observed giant branches, which are strongly curved and very shallow for metal rich clusters. We also note a possible gap near  $K \sim 12.7$  within the giant branch of this cluster.

Data from Frogel (1985) can be compared with ours in an indirect way. Direct comparison is not possible because all of their stars fall outside our field centered on the cluster center. The locations of their stars overlaid on our near-infrared CMD confirm that our photometry is in general agreement with their photometry.

## IV. SLOPE OF GIANT BRANCH STARS AND METALLICITY

Stellar interior calculations show that the slope of giant branch is sensitive to the metallicity of a cluster, while insensitive to its age (Green 1987). Kuchinski & Frogel(1995) confirmed this and derived an empirical relationship between globular cluster's metallicity

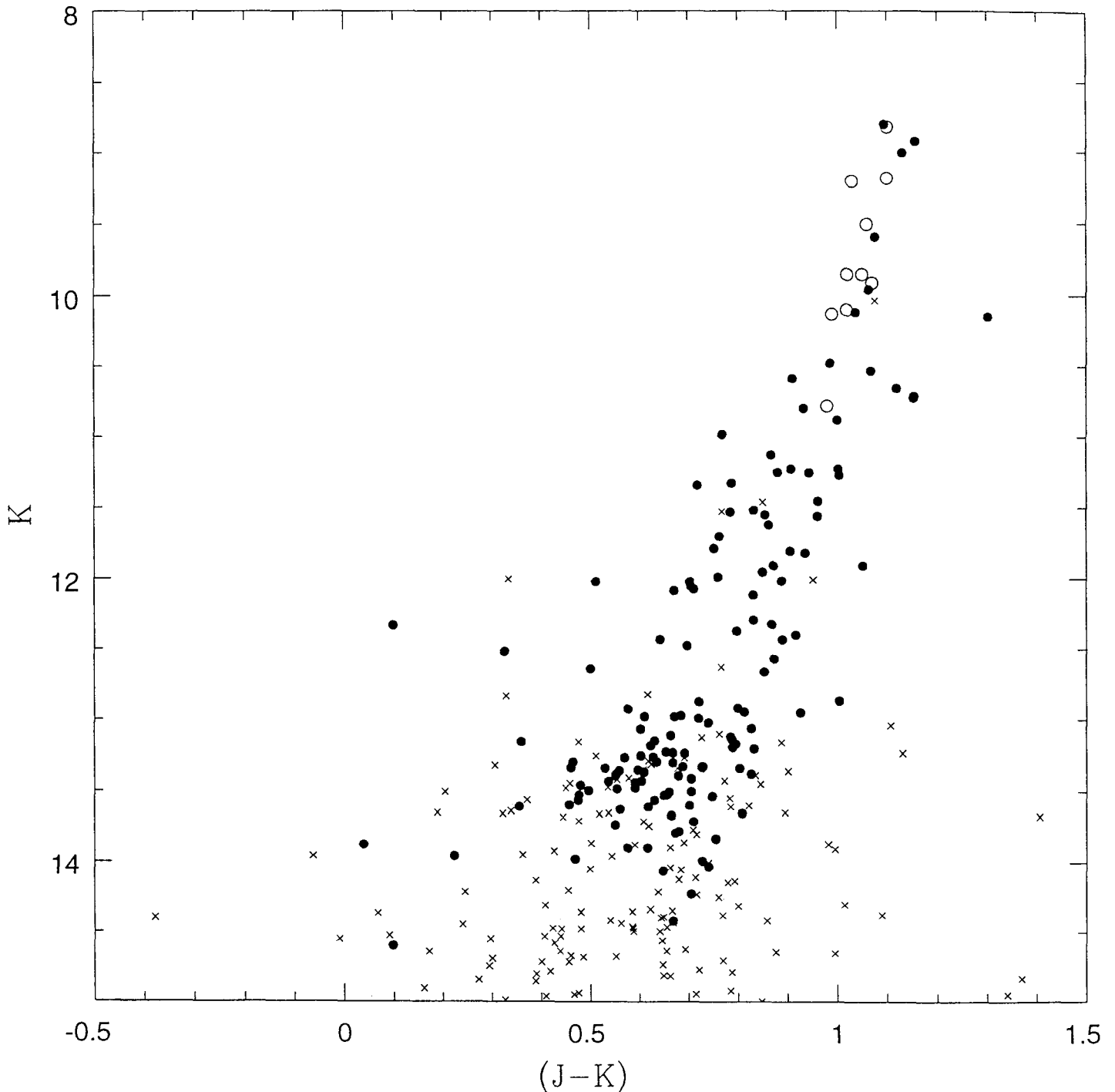


**Fig. 2.**—  $(K, J - K)$  CMD of NGC6712. Cross represent stars with photometric errors less than 0.06, dot greater than 0.06. We can see the gap near  $K \sim 12.7$ . We compare with Frogel(1985)'s photometric data(filled circle).

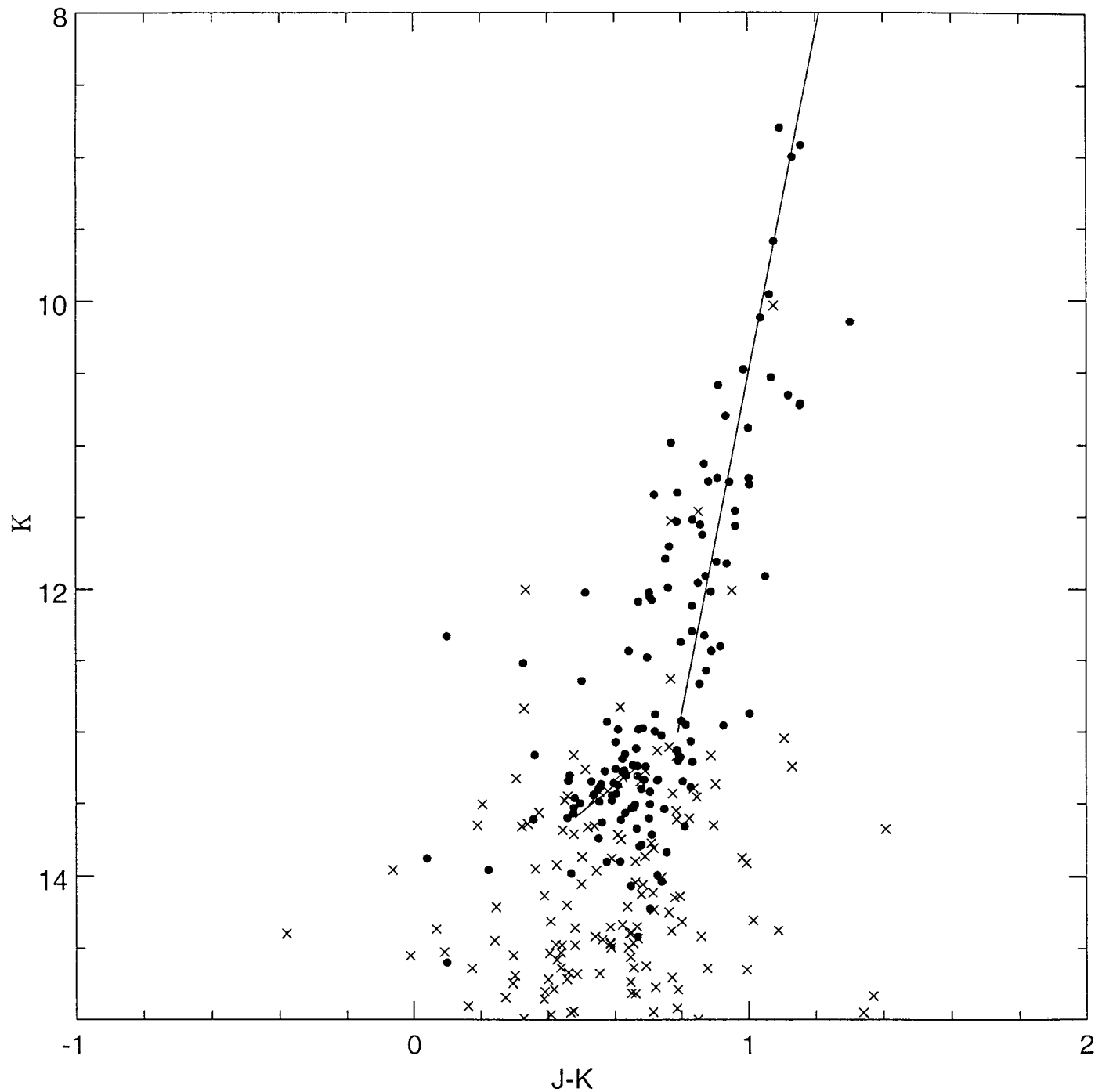


Fig. 3.— ( $K, J - K$ ) Slope fit to the giant branch star of NGC6712. We excluded stars which are probable asymptotic giant star.

**Table 3.** Giant branch slope and the related parameter of NGC6712.

$\chi(J - K)^a$	a	b	[Fe/H]	<sup>b</sup>
$\pm 0.04$	$1.89(\pm 0.06)$	$-0.085(\pm 0.005)$	-0.96	ours
$\pm 0.06$	$1.97(\pm 0.06)$	$-0.095(\pm 0.006)$	-1.01	data1
$\pm 0.05$	$1.88(\pm 0.06)$	$-0.087(\pm 0.005)$	-1.01	data2

<sup>a</sup> $\chi(J - K)$  is a fitting error

<sup>b</sup>data1 is Kuchinski *et al*(1995)'s LCO data

data2 is Kuchinski *et al*(1995)'s OSIRIS data

[Fe/H] and their near-infrared giant branch slopes using several clusters.

$$[\text{Fe}/\text{H}] = -3.06(\pm 0.81) - 24.63(\pm 8.06) \times (\text{GB slope})$$

The uncertainty in a value of [Fe/H] due to the scatter of the values that into the derivation of this relation is  $\pm 0.25$  dex. We made a linear fit to giant branch stars brighter than the horizontal branch over the range  $13.2 > K > 8.0$ . The fit was made iteratively; those outlying stars with locations more than  $2\sigma$  away from the best fit were eliminated after each iteration. We also excluded stars which appear to be in the stage of asymptotic giant. The fitting error( $\chi(J - K)$ ), the derived slope(b), and the uncertainty in the slope are given in Table 3. The best fit line, uncorrected for reddening, is also shown in Fig. 3. The slope of giant branch in a near-infrared CMD does not depend on the reddening. The slope and the related parameter of NGC6712 giant branch star we derived are very similar to the result of Kuchinski *et al*(1995)(see Table 3). Based on the slope, we obtained its metallicity  $[\text{Fe}/\text{H}] \sim -0.96$  from the above equation. Our value is in accordance with Zinn & West(1984)'s metallicity estimated by optical method and also with Frogel(1985)'s estimate using CO indices.

The distance to clusters with IR data only can be determined by comparing the observed level of horizontal branch in  $K$  with the known absolute level  $M_{K_0}(\text{HB}) = -1.15 \pm 0.09$ (Kuchinski *et al*(1995)). We obtained the center magnitude of HB level as  $m_{K_0} = 13.35 \pm 0.12$  using  $E(B-V)=0.48$  (Sandage & Smith 1966),  $A_V=3.12E(B-V)$ , and  $E(J-K)=0.56E(B-V)$  (Bessel & Brett 1988) calculated from the regression line in Fig. 3. The derived distance modulus for NGC6712 is  $(m-M)= 13.42 \pm 0.12$ .

## V. SUMMARY

In this paper, we present the JK photometric data for the central region of NGC6712 resulted from our near-infrared observations. The near-infrared CMD of

this cluster is very similar to the CMDs of other metal-rich globular clusters with a linear and very steep giant branch. Using the well-established relation between the slope of giant branch and its metallicity, we derived the metallicity of  $[\text{Fe}/\text{H}] \sim -0.96 \pm 0.27$ . The slope of giant branch is similar to the one Kuchinski *et al*(1995) derived from near-IR observation data. The distance to NGC6712 has been estimated using the level of the horizontal branch and is  $13.42 \pm 0.12$  in distance modulus. This distance is somewhat smaller than previously available estimates, for example, 14.16(Frogel *et al* 1983).

We would like to thank the observatory staffs at the Mauna Kea branch of the University of Hawaii for their assistance during our observing run. We were supported by the Korean Ministry of Science and Technology (MOST) through Star Project (No. 97-1-300-00). YIB also acknowledges the support from the Creative Research Initiatives Program of MOST as well as the support from Yonsei University.

## REFERENCES

- Armandroff, T. E. and Zinn, R. 1988, AJ, 96, 92
- Bessell, M. S. and Brett, J. M. 1988, PASP, 100, 1134
- Cudworth, K. M. 1988 AJ, 96, 105
- Frogel, J. A., Persson, S. E. and Cohen, J. G. 1983, ApJS, 53, 713
- Frogel, J. A. 1985, ApJ, 291, 581
- Green, E. M., Demarque, P. and King, C. R. 1987, Revised Yale Isochrone and Luminosity Functions (Yale Univ. Obs., New Haven).
- Hodapp, K.-W., Rayner, J. and Irwin, E. 1992, PASP, 104, 441
- Kuchinski, L. E., Frogel, J. A. 1995, AJ, 110, 2844
- Kuchinski, L. E., Frogel, J. A., and Terndrup, D. M. 1995, AJ, 109, 1131
- Kyeong, J., Byun, Y-I and Chun, M. S. 1997, JKAS, 30, 123

- Sandage, A. and Smith, L. L. 1966, ApJ, 144, 894  
Stetson, P. B. and Harris, W. E. 1988, AJ, 96, 909  
Zinn, R. J. and West, M. J. 1984, AJ, 293, 424